Fusion of Reconstructed Multispectral Images

Valery Starovoitov
Institute of Computer Science
University of Bialystok
Bialystok, Poland,
United Institute of Informatics Problems
Minsk, Belarus
valerys@newman.bas-net.by

Aliaksei Makarau
United Institute of Informatics Problems
Minsk, Belarus
makarau@newman.bas-net.by

Igor Zakharov and Dmitry Dovnar
Institute of Technology of Metals
Mogilev, Belarus
zakharov@ieee.org, dovnar@inbox.ru

***Abstract*—A new technique for fast fusion of multiresolution satellite images with minimal colour distortion is presented in the paper. The technique allows to reconstruct multispectral images with resolution higher than resolution of the panchromatic image. Combination of image super-resolution restoration and image fusion based on global regression was applied. Super-resolution image restoration is based on simultaneous processing of several multispectral images to reconstruct a panchromatic image with higher resolution. This method is quasi-optimal on minimum squared errors of image restoration.**

Image Fusion, Image Restoration, Super-resolution

I. INTRODUCTION

Image fusion or pan-sharpening is performed in order to increase resolution of multispectral images utilizing the panchromatic image information. Resolution of sharpened images is limited by resolution of a panchromatic image. For example, Landsat 7ETM+ provides panchromatic images with resolution 15m and multispectral with 30m. Therefore, resolution of the sharpened multispectral images is two times higher than original one. The Brovey transform [1] and IHS fusion [2] methods are point type methods, fast and applicable for images of the large size. PCA and wavelet-based fusion methods [3] are of global and local operator type and computationally expensive. In satellites launched after 1999, sensitivity range of the panchromatic image sensor is usually extended to cover nearest infrared range. It is made in order to increase resolution of the registered panchromatic image, but previously developed fusion methods cause significant color distortion [4].

We develop a principally new technique for multispectral image fusion with resolution higher than resolution of the panchromatic image and with minimization of color composite distortion. Two tasks are to be solved in order to achieve the higher resolution: panchromatic image reconstruction (super-resolution) and multispectral image fusion.

To solve the first task one can use reconstruction of a panchromatic image from color images by demosaicing algorithm [5] either super-resolution reconstruction [6]. Our solution is based on the method, which is quasi-optimal on minimum squared error (MSE) of image restoration [7]. This method allows a theoretical quality evaluation and super-resolution restoration from several images. The solution of the second task may be based on an algorithm of multiresolution image fusion. We select a fusion algorithm based on the linear regression. The algorithm is of point type (*i.e.* fast) and provides minimal color composite distortion.

The restored panchromatic and original panchromatic images were compared using the structural similarity index (SSI) from [8]. Quality of enlarged images we evaluated by the Euclidean norm (L2) of the histogram difference of the original and the fused images, correlation, RMSE, square error of the difference image (SEDI).

II. IMAGE RESTORATION METHOD

The optimal solution of Fredholm's integral equation of the first kind may be used for image resolution increase [7]. Note, that images are registered by a focal plane array (FPA).

A. Model of Image Formation

Information about optical properties of the original ideal image $Z(\xi,\eta,\lambda)$ is transmitted into an optical system, which is characterized by a point-spread function (PSF) $K(x,y,\xi,\eta,\lambda)$. The optical system projects an image $f(x,y,\lambda)$ onto the FPA. This process can be described by a linear equation

$$f(x,y,\lambda)=\int_{-S_1}^{S_1}\int_{-S_2}^{S_2} Z(\xi,\eta,\lambda)K(x,y,\xi,\eta,\lambda)d\xi d\eta, \qquad (1)$$

where S_1, S_2 are integration limits, (ξ,η) are the coordinates of a point in the plane of image $Z(\xi,\eta,\lambda)$, λ is the wavelength of light, (x,y) are the coordinates of point in the plane of the registered image $f(x,y,\lambda)$. The images with different spectral bands and light wavelengths in (1) are labeled by $f(x,y,\lambda_p,p)$, where $p=0,1,...P$, $\lambda_p=\lambda_0,\lambda_1,...\lambda_P$.

Spectral photosensitivity function $Sen(x,y,\lambda)$ of an FPA element can be non-uniform [9]. The fill factor of FPA may be

The work was partly supported by INTAS project No.: 06-1000024-9100.

known from the manufacturer to describe the function. Registration of the ideal image $Z(\xi,\eta,\lambda)$ can be described by Fredholm's integral equation. For the image $f(i,j,p)$ registered by FPA the equation is

$$\int_{-S_1}^{S_1}\int_{-S_2}^{S_2} Z(\xi,\eta,\lambda)K_1(i,j,\xi,\eta,\lambda_p,p)d\xi d\eta = \\ = f(i,j,p)+\gamma(i,j,p) = F(i,j,p), \tag{2}$$

where

$$K_1(i,j,\xi,\eta,\lambda_p,p) = \\ = \iint_{A_{i,j}} Sen(x,y,\lambda)K(x,y,\xi,\eta,\lambda,p)dxdy, \tag{3}$$

$F(i,j,p)$ – signal registered by an FPA (i,j) element with area $A_{i,j}$, λ_p – the light wavelength for image p, $\gamma(i,j,p)$ – error of the signal (additive noise). We can write

$$F(i,j,p) = \iint_{A_{i,j}} Sen(x,y,\lambda_p)f(x,y,\lambda_p,p)dxdy + \\ + \gamma(i,j,p). \tag{4}$$

Hence, the function *K* (PSF) in (3) can be written as

$$K(x,y,\xi,\eta,\lambda,p) = \begin{cases} K(x,y,\xi,\eta,\lambda_0), p=0, \\ K(x,y,\xi,\eta,\lambda_1), p=1, \\ \ldots\ldots\ldots\ldots\ldots\ldots \\ K(x,y,\xi,\eta,\lambda_P), p=P. \end{cases} \tag{5}$$

B. Solution of the Integral Equation

Solution of (1) is an ill-posed problem. According to the theory of regularization, small errors (noise) $\gamma(i,j,p)$ can lead to huge dispersion in solution of the equation. It is possible to build an approximated solution with regularized properties. Let us consider an approximated stabilized solution. It is possible to find the average value over the set of squared error of restoration. The solution can be represented as decomposition on arbitrary orthonormalized system of basic functions $\psi_k(\xi,\eta,\lambda)$:

$$Z(\xi,\eta,\lambda) = \sum_{k=1}^{\infty} c_k\psi_k(\xi,\eta,\lambda), |\xi| < S_1, |\eta| < S_2, \tag{6}$$

where c_k are the decomposition coefficients. The initial image *Z* and noise are non-correlated.

In comparison to Wiener method, the main advantage of the presented image restoration method is calculation of the MSE for small number of pixels in the initial image. This is very important for reconstruction of image registered by FPA [10]. Values of a signal $F(i,j,p)$ are used for restoration $Z^*(\xi,\eta,\lambda)$ of the ideal continuous image Z. An algorithm described in [7] was adopted for this restoration. This algorithm is fast, but in comparison with blind image restoration methods (e.g. [11]) has a disadvantage – the PSF is to be known. Image restoration filter $Q(\xi,\eta,i,j,p,\vec{\beta})$ can be calculated by equations in [10]. The filter is calculated using stabilization parameters $\vec{\beta} = (\beta_1,\beta_2,...)$ by the equation:

$$Q(\xi,\eta,i,j,p,\vec{\beta}) = \\ = \sum_{m=1}^{G} \frac{\sum_{k=1}^{m} d_{km}(\vec{\beta})\varphi_k(i,j,p)\sum_{k=1}^{m} d_{km}(\vec{\beta})\psi_k(\xi,\eta)}{\beta_m + \sum_{k=1}^{m} d_{km}(\vec{\beta})(\varphi_k,\varphi_m)}, \tag{7}$$

where $(\varphi_k,\varphi_m) = \sum_i^I \sum_j^J \varphi_k(i,j)\varphi_m(i,j)$ are scalar multiplication of images of basis functions, *G* is number of functions of object decomposition, *I* x *J* is the number of pixels, $d_{ln}(\vec{\beta})$ are recurrently calculated coefficients

$$\begin{cases} d_{\ln}(\vec{\beta}) = -\sum_{m=l}^{n-1} d_{lm}(\vec{\beta}) \dfrac{\sum_{k=1}^{m} d_{km}(\vec{\beta})(\varphi_k,\varphi_m)}{\beta_m + \sum_{k=1}^{m} d_{km}(\vec{\beta})(\varphi_k,\varphi_m)}; \\ l = 1,2,...,n-1; n = 2,3,...; d_{kk}(\vec{\beta}) = 1, k = 1,2,.... \end{cases} \tag{8}$$

Summation is made over all sampling points of an image $F(i,j,p)$ for the original image restoration

$$Z^*(\xi,\eta,\lambda) = \sum_{i,j,p} F(i,j,p)Q(\xi,\eta,i,j,p,\vec{\beta}) \tag{9}$$

Knowledge of the PSF (5) is required for restoration based on different spectral images.

Image restoration algorithm

Step 1. Enter images $F(i,j,p)$, $p = 0,1,...P$. Enlarge the images by interpolation.

Step 2. Set parameters of the FPA: fill factor or $Sen(x,y,\lambda)$, SNR, enter values of the PSF $K(x,y,\xi,\eta,\lambda_p,p)$ for every image.

Step 3. Calculate a filter $Q(\xi,\eta,i,j,p,\vec{\beta})$ and reconstruct an image Z^* by (9).

III. Multispectral Image Fusion Using Global Regression

Hill et.al. proposed an algorithm for multiresolution image fusion [12]. The algorithm calculates local regression in a sliding window with size $n \times n$ (*n*=5 in [12]) between degraded

(Pan^{deg}) and scaled (Pan^{low}) panchromatic and the spectral image. Local regression analysis between the image Pan^{low} and the spectral image $Mult_j$ is calculated by

$$Mult_j = A_j + B_j * Pan^{low} + E_j . \quad (10)$$

A_j, B_j are the matrices of local regression parameters for the j-th spectral image, E_j is the matrix of residuals, Pan^{low} is the degraded and scaled down panchromatic image. The spectral image $Mult_j$ and the matrix B_j are resized to the size of the panchromatic image by interpolation (entitle results as $Mult_j^h$ and B_j^h). The spectral image with high resolution is calculated by

$$Mult_j^{high} = Mult_j^h + B_j^h (Pan - Pan^{\deg}), \quad (11)$$

where $Mult_j^{high}$ is high resolution spectral image. This algorithm is a local type algorithm, computationally expensive. Keeping the matrix B_j^h, which size is equal to the size of the panchromatic image, is costly in memory.

Distribution of the local regression parameters B_j of Landsat 7 ETM+ images was analyzed. Median values of B_j for all spectral images and coefficients of the global linear regression are very close. Since, the median values are close to the coefficients of the global regression, the global regression may be applied for multiresolution image fusion.

Algorithm for multiresolution image fusion based on global regression

Input data: $Mult_j$ is the spectral image, *Nir* is the near infrared image, *Pan* is the panchromatic image.

Step 1. For the $Mult_j$ and Pan images assign zero values for the pixels representing cloud, water and shadow areas. The mask can be calculated by the following formulas

$$\begin{aligned} &Mask(1..M,1..N) = 1, \quad then \\ &Mask(B > T_B) = 0; Mask(Nir < T_{Nir}) = 0, \end{aligned} \quad (12)$$

where M,N is the size of the image, B is spectral image of blue color range, *Mask* is the mask with zero pixels representing water, shadow and cloud areas, T_B and T_{Nir} are the thresholds for the B and the *Nir* images. The thresholds T_B and T_{Nir} were calculated experimentally (200 and 40 for Landsat 7 ETM+).

Step 2. Degrade the *Pan* image by a low-pass filter (3×3 average filtering, for example), entitle as Pan^{deg}. Scale down Pan^{deg} to the size of the spectral image by interpolation (entitle as Pan^{low}).

Step 3. Calculate the global regression coefficients

$$Mult_j = a_j + b_j * Pan^{low} + E_j , \quad (13)$$

where a_j and b_j are the global regression parameters, E_j is the residuals matrix.

Step 4. Perform spatial scaling of the $Mult_i$ image to the size of the panchromatic image (entitle the result as $Mult_j^{'}$).

Step 5. Increase resolution of the spectral image by

$$Mult_j^{''} = Mult^{'} + b_j * (Pan - Pan^{\deg}), \quad (14)$$

where $Mult_j^{''}$ is the spectral image with increased resolution. Assign 0 or 255 to the pixels of the fused image, which values are less than 0 or more than 255, respectively.

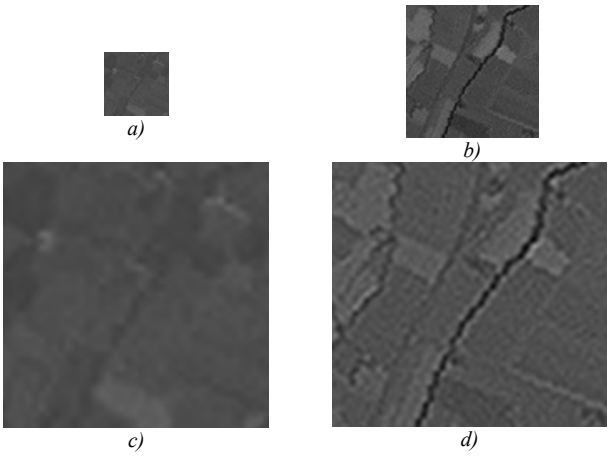

Figure 1. Example of image restoration from multispectral images: *a)* a fragment of red spectrum image; *b)* the fragment of the panchromatic image; *c)* interpolated image of red spectrum; *d)* image reconstructed from multispectral, near infrared and panchromatic images.

IV. Results of Algorithms Evaluation

A. Image Restoration Results

Fig. 1 (a) and (b) illustrate fragments of red spectrum image and original panchromatic image. Fig. 1 (*c*) presents interpolated image of red spectrum. Fig. 1 (*d*) presents restored image using multispectral, near infrared and panchromatic images.

B. Quality Assessment of Image Restoration Results

The restored image was compared with interpolated spectral and interpolated panchromatic images by calculation of correlation, RMSE, square error of the difference image (SEDI) and structural similarity (see Table 1). The restored image has bigger correlation with the interpolated *Nir* image than with other images. Utilization of the *Nir* image for *Pan* image restoration is desirable.

TABLE I. Comparison of Interpolated Spectral Images with the Restored Image Shown in Fig. 1(d)

Interpolated image	Correlation	RMSE	SEDI	SSI
Pan	0.988	18694	4.15	0.88
R	0.143	42481	13.33	0.59
G	0.231	52519	24.19	0.56
B	0.390	40564	16.76	0.62
Nir	0.949	45185	11.01	0.60

C. Image Fusion Results

Results of the presented algorithm were compared with the Brovey, IHS and local regression fusion methods. Spectral

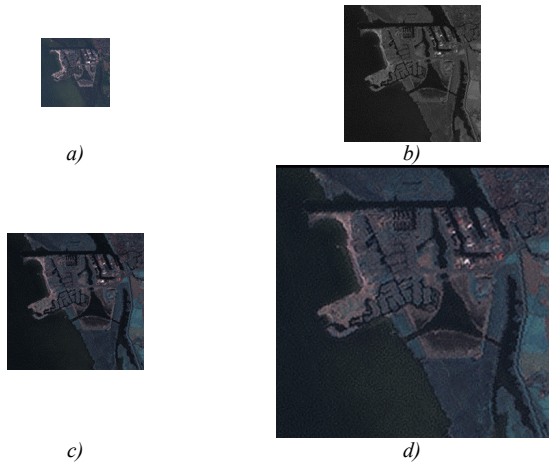

Figure 2. Fusion by different methods: *a)* a fragment of an original multispectral image (Landsat 7 ETM+); *b)* the panchromatic image, *c)* the IHS fusion with original panchromatic image; *d)* the IHS fusion with reconstructed panchromatic image.

images with size of 400×400 pixels and restored panchromatic images with size 1600×1600 pixels were used. Fig. 2 presents (*a*) a fragment of a multispectral image, (*b*) the original panchromatic image, (*c*) the IHS fusion, (*d*) the IHS fusion with restored panchromatic image (the resolution is 4 times higher then the resolution of the multispectral image, and 2 times higher than the resolution of the panchromatic image).

TABLE II. NUMERICAL EVALUATION OF THE FUSION METHODS. THE ORIGINAL MULTISPECTRAL IMAGE OF SIZE 400×400, THE FUSED IMAGE OF SIZE 1600×1600 PIXELS.

Method	L2 histogram Norm (R,G,B)	Correlation (R,G,B)	RMSE (R,G,B)	SEDI (R,G,B)	Consumed time, s
Brovey Fusion	31045 32443 42114	0.5294 0.3384 0.0189	7654 12144 12247	9.9783 10.0945 14.0574	16.171
IHS Fusion	162152 162610 164330	0.1101 0.0889 0.1409	21578 25116 29445	16.3232 9.91 7.8131	**13.844**
Local regression	**3328** **2643** **4258**	**0.9858** **0.9851** 0.9738	**1151** **704** 744	**1.9249** 1.1786 1.2391	77.703
Global regression	3372 2785 4604	**0.9858** **0.9851** **0.9744**	1157 **704** **739**	1.9376 **1.1855** **1.2348**	15.578

D. Visual Analysis

All the discussed algorithms increase the spatial resolution, but the Brovey and IHS fusion methods heavily distort the color composite. Visually there is no color distortion in the local and global regression fusion results, but the local regression fusion adds noise near edges and in the homogeneous areas in the resulting image.

E. Quantitative Analysis

The Euclidean norm (L2) of the histogram difference of the original and the fused images, correlation, RMSE, square error of the difference image (SEDI) were used in quantitative analysis. The fused images were scaled down to the size of the original multispectral images by bilinear interpolation. Ideal values for all the measures are 0, but for correlation is 1. Table 2 presents assessment of image fusion by the Brovey, IHS, local and global regression fusion. Size of the original multispectral image is 400×400 pixels. Size of the fused images is 1600×1600 pixels. The best values are indicated by bold font. Fusion based on the local and global regression outperforms widely used the Brovey and IHS fusion methods. Calculation time of the global regression fusion is less than calculation time of the Brovey fusion and comparable to the IHS fusion. Experiments were carried out in Matlab R14.

V. CONCLUSION

We presented a new technique for multispectral image fusion with minimization of color composite distortion. The resolution of the fused image is higher than resolution of the original panchromatic image. This was done in two stages: by super-resolution of panchromatic image using the original multispectral and panchromatic images; then multispectral image fusion with the reconstructed panchromatic image. This allows to increase resolution of the image 2-4 times higher than the original panchromatic image resolution without loss of acutance and color composite distortion.

REFERENCES

[1] Y. Zhang, "Problems in the fusion of commercial high resolution satellite images as well as Landsat 7 images and initial solutions," Joint Int. Symposium on GeoSpatial Theory, Processing and Applications, Ottawa, Canada, July 2002, vol. 34, part.4.

[2] T. Tu, S. Su, H. Shyu, and P. Huang "A new approach at IHS-like image fusion methods," Information Fusion, vol. 2, no. 3, pp. 177–186, 2001.

[3] Z. Wang, D. Ziou, C. Armenakis, D. Li, and Q. Li, "A comparative analysis of image fusion methods," IEEE Trans. Geoscience and Remote Sensing, vol. 43, no. 6, pp. 1391–1402, 2005.

[4] T. Tu, Y. Lee, C. Chang, and P. Huang "Adjustable intensity-hue-saturation and Brovey transform fusion technique for IKONOS/Quickbird imagery," Optical Engineering, vol. 44, no. 11, pp. 116201-1–116201-10, 2005.

[5] R. Kimmel, "Demosaicing: Image reconstruction from color CCD samples," IEEE Trans. Image Proc., vol. 8, no. 9, pp. 1221–1228, 1999.

[6] R. Molina, J. Mateos, and A. Katsaggelos "Super resolution reconstruction of multispectral images," VIRTUAL OBSERVATORY: Plate Content Digitization, Archive Mining & Image Sequence Processing, Heron Press, 2005.

[7] D. Dovnar and K. Predko, "The method for digital restoration of object distorted by linear system," Acta Polytechnica Scand. Applied Physics Series, vol. 1, no 149, pp. 138-141, 1985.

[8] Z. Wang and A. Bovik "A universal image quality index," IEEE Signal Proc. Letters, vol. 9, no. 3, pp. 81-84, 2002.

[9] D. Kavaldiev and Z. Ninkov, "Influence of nonuniform charge–coupled device pixel response on aperture photometry," Optical Engineering. vol. 40, no. 2, pp. 162–169, 2001.

[10] D. Dovnar and I. Zakharov "The orthogonalization method for error compensation of Wiener filter for spatial discreditized images," in Proc. 8th Int. Conf. on Pattern Recognition and Information Proc., Minsk, Belarus, May 2005, pp. 173–176.

[11] R. Molina, J. Mateos, and A. Katsaggelos "Blind deconvolution using a variational approach to parameter, image, and blur estimation," IEEE Trans. on Image Processing, vol. 15, no. 12, pp. 3715-3727, 2006.

[12] J. Hill, C. Diemer, O. Stover, and T. Udelhoven. "A local correlation approach for the fusion of remote sensing data with different spatial resolution in foresty applications," in Proc. of Int. Archives of Photogrammetry and Remote Sensing, Valladolid, Spain, June 1999, vol. 32, no. Part 7-4-3 W6, pp. 167–174.